RSC Advances

ROYAL SOCIETY OF CHEMISTRY

www.rsc.org/advances

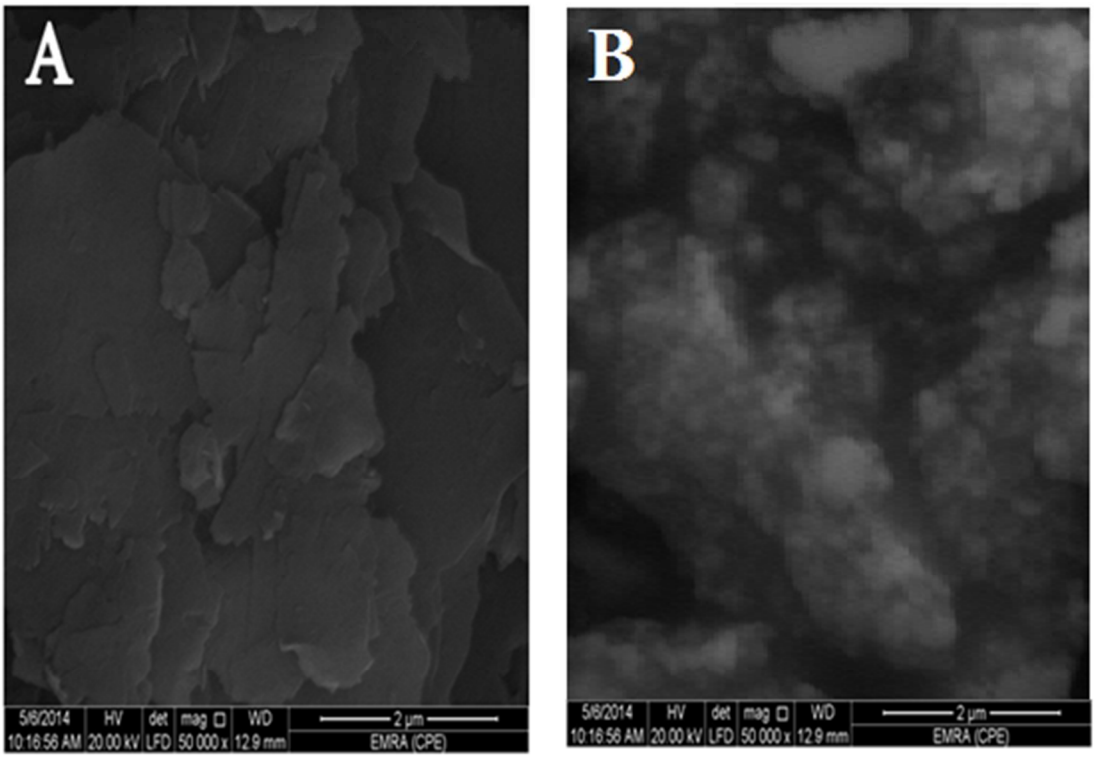

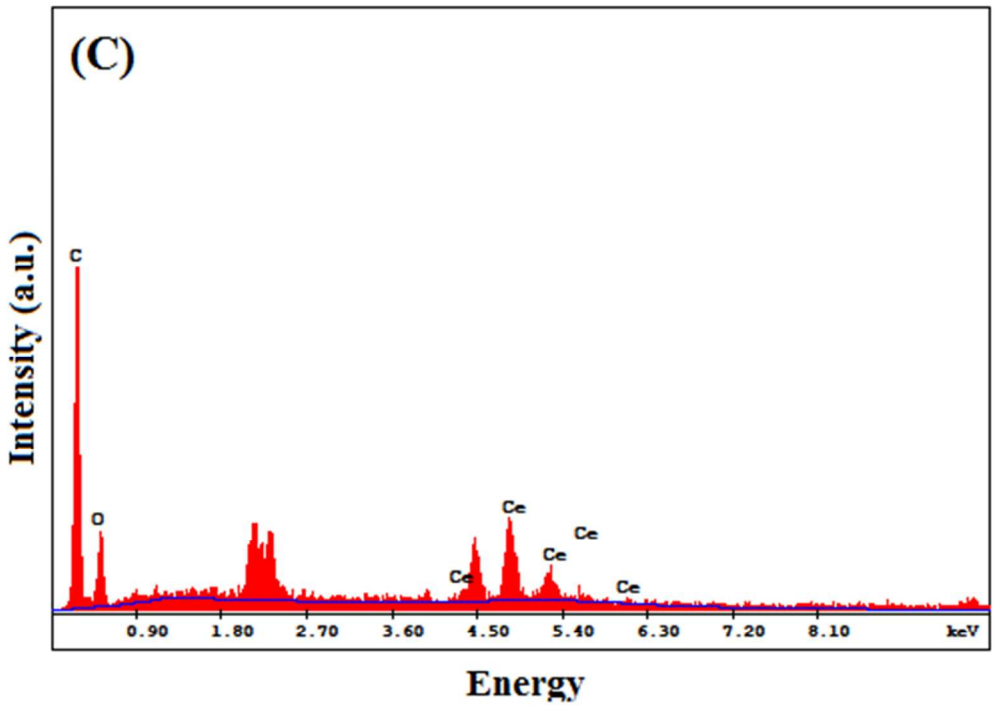

A Novel electrochemical nicotine sensor based on cerium nanoparticles with anionic surfactant

A.M. Fekry[a], S.M. Azab[b], M. Shehata[a], M.A. Ameer[a*]

[a]*Chemistry Department, Faculty of Science, Cairo University, Giza-12613, Egypt.*
[b] *Pharmaceutical Chemistry Dept., National Organization for Drug Control and Research [NODCAR], 6 Abu Hazem Street, Pyramids Ave, Giza-29, Egypt*

Abstract

A novel promising electrochemical nicotine (NIC) sensor was done by electrodeposition of Ce-Nanoparticles on a carbon paste electrode (CPE). The work was done using electrochemical techniques including cyclic voltammetry (CV), electrochemical impedance spectroscopy (EIS), Scanning electron microscope (SEM) and *Energy Dispersive X-Ray Analysis* (EDX) techniques, in both aqueous and micellar media. NIC Measurements were investigated in Britton-Robinson (B-R) buffer solution of pH range (2.0-8.0) containing (1.0mM) sodium dodecylsulfate (SDS). The linear response range of the sensor was between 4×10^{-6}M and 5×10^{-4}M with a detection limit of 9.43×10^{-8}M. Good satisfactory results were achieved for the detection of NIC in real samples and different brands of commercial cigarettes.

Keywords: Nicotine; Ce Nanoparticles; EIS; SEM; EDX.

*Corresponding author: E-mail: mameer_eg@yahoo.com

1. Introduction

Nicotine, 3-(1-methyl-2-pyrrolidinyl) pyridine, is the main alkaloid in tobacco leaves (Nicotiana tabacum L., Solanaceae), the latter being best known for their use in cigarettes rather than for their therapeutical applications.[1,2] Nicotine (scheme 1) is one of the most heavily used addictive substances ever available. Pharmacologically nicotine is a compound which acts on central nervous system in form of elevation of mood, sense of euphoria and revitalizing energy but it has some very potential health hazard primary being the cardiovascular and respiratory disorder including lungs cancer. Apart from its harmful effects, studies have also been carried out to know its medicinal value with the disease like ulcerative colitis, Alzheimer's and Parkinson's diseases.[3] Moreover, the nicotine determination is an important analysis for the tobacco industry, since the quality of the product can be determined by its nicotine content, which varies with tobacco type, but the normal nicotine level range goes from 1% to 3%.[1,4] Thus, its determination is important in medicine, toxicology and tobacco industry. At the past, there has been considerable interest in the development of methods for nicotine determination including spectrophotometry,[5] chromatography,[6] reversed HPLC,[7] and potentiometry.[8,9] Some of these methods require preliminary extraction and purification of nicotine from the sample matrix and skilled personnel manipulating sophisticated instrumentation,[3] leading to considerable losses of the analyte to be determined. From the electrochemical considerations, not many detection studies have been made on this compound. This is mainly because the nicotine oxidation/reduction processes occur at extremely positive/ negative potentials, which are out of the potential window of the conventional electrodes.[1] Suffredini et al. made a progress at the area of nicotine peak separation using a boron-doped diamond electrode in basic media.[10] Hannisdal et al. investigate the

electroreduction of nicotine on dropping mercury electrode to perform its quantification in chewing gum, patches and tablets.[11] Amperometric assay based on nicotine inhibition biosensors were applied and provided a promising approach to the determination of nicotine in tobacco.[12] Amperometric detection of nicotine also studied on a titanium dioxide/poly(3,4-ethylenedioxythiophene) modified electrode by a molecular imprinting technique.[13] Lin et al. described a flow injection-electrochemiluminescent method based on tri(2,2-bipyridyl)ruthenium (II) complex system for the nicotine quantification.[14] Marcus et al. also studied the effects of thin-layer diffusion in the electrochemical detection of nicotine on basal plane pyrolytic graphite (BPPG) electrodes modified with layers of multi-walled carbon nanotubes (MWCNT-BPPG).[15] Tar Wu et al. made a detection for nicotine using molecularly imprinted TiO2-modified electrodes.[16] Recently a sensitive determination of nicotine in tobacco products and anti-smoking pharmaceuticals reached using boron-doped diamond electrochemical sensor.[17] In this work, we introduce a sensitive electrochemical procedure for NIC detection based on Cerium nanoparticles modified carbon paste electrode (CNMCPE) that can overcome obstacles facing conventional electrodes . Due to its low cost, high sensitivity for detection, low background current, ease of fabrication and renewable surface, carbon paste electrode has been widely used for the electroanalytical applications.[18] Nanoparticles research is advancing at a fast place due to their unique properties, such as having increased electrical conductivity, toughness and ductility, increased hardness and strength of metals and alloys. Electrodeposition of Ce-nanoparticles on CPE surface was an important method for detection of NIC. Ce nanoparticles showed a large participation in the area of electrochemical sensors, biosensors[19] and batteries.[20]

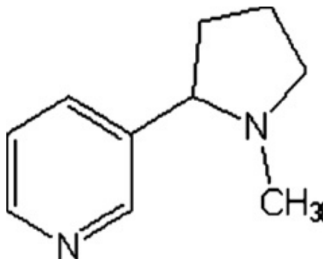

Scheme 1: Chemical structure of nicotine.

Surfactants have been widely used in chemistry and have proven to be effective in the electroanalysis of biological compounds and drugs. The use of surfactant solutions as modifiers improve the sensitivity and selectivity of the voltammetric measurements.[1]

To our knowledge, there is no work been made using CP-Ce nanoparticles sensor for the determination of nicotine using anionic surfactant, so the aim of this work is to construct a novel and sensitive electrochemical sensor based on Ce nanoparticles, graphite and SDS to be used for the determination of nicotine in urine samples and cigarettes.

2. Experimental

2.1. Reagent and chemicals

Nicotine standard samples (99%) were provided by Egyptian Eastern Company for Smoking and were used as received without prior purification. Nicotine stock solutions of about 1.62 g/L were freshly prepared in water then stored in a dark container since the compound is sensitive to light. Supporting electrolyte, namely, Britton–Robinson (B–R) (4.0×10^{-2} M) buffer solution of pH 2.0–8.0 (CH_3COOH + H_3BO_3 + H_3PO_4) were used for preparing the standard solutions of nicotine. pH values were adjusted using 0.2 M NaOH. Sodium dodecylsulfate (SDS) was purchased from sigma Aldrich. All solutions were prepared from analytical grade chemicals and triply distilled water. Cigarette samples were purchased from the local

supermarkets. Two products of different international cigarette brands: L&M® and Marlboro® were chosen. All experiments were carried out at the room temperature of the laboratory for 2-3 times and gave reproducible results.

2.2. Preparation of Cerium nanoparticles modified CP electrode (CNMCPE)

Carbon paste electrode (CPE) with a diameter of 3 mm was prepared using few drops of paraffin oil mixed with graphite powder (0.5g) and the mixture was blended thoroughly to obtain a homogeneous paste.[21] The resulting mixture was used to fill into a Teflon tube and pressed tightly. The CPE was polished with ultra fine emery paper until a smooth surface was achieved. CPE surface was pre-treated by applying a potential of +1.3V for 30 s in the blank supporting electrolyte without stirring, in order to increase the hydrophilic properties of the electrode surface through introduction of oxygenated functionalities, accomplished with an oxidative cleaning. Ce nanoparticles modified CPE was formed by dipping the clean CPE into 0.1 mM ammonium ceric nitrate solution, about 2 ml lactic acid and the solution pH was adjusted using (33 %) ammonium hydroxide solution and then scanning the electrode in the potential range from −2.0 to +2.0 V at 25 mV/s for 5 cycles in the prepared solution at 25 °C.[22]

2.3. Electrochemical measurements

All electrochemical measurements were investigated using electrochemical IM6e Zahner-elektrik, GmbH, (Kronach, Germany) workstation. A typical three-electrode fitted with a large platinum sheet of size 15×20×2mm as a counter electrode (CE), saturated calomel electrode (SCE) as a reference electrode (RE) and CNMCPE as the working electrode (WE) were used. A HANNA 213 pH meter with glass combination electrode was used for pH measurements.

Scanning electron microscopy (SEM) measurements were carried out using SEM Model Quanta 250 FEG (Field Emission Gun) attached with EDX Unit (Energy Dispersive X-ray Analyses), with accelerating voltage 30 K.V., magnification14x up to 1000000 and resolution for Gun.1n) (FEI company, Netherlands) .

All the electrochemical experiments were carried out and repeated for 2-3 times at room temperature of 25 °C and gave reproducible results.

2.4. Impedance spectroscopy measurements.

Electrochemical impedance spectroscopy (EIS) was carried out using the electrochemical workstation IM6e Zahner-elektrik, GmbH, (Kronach, Germany). All impedance experiments were recorded between 0.1 Hz and 100 kHz at 10 mV amplitude. Analyses of the experimental spectra were made using Thales software provided with the workstation.

2.5. Analysis of urine

Standard NIC provided by Egyptian Eastern Company for Smoking was dissolved in urine (diluted 400 times using 100 ml of B–R buffer pH 2) to make a stock solution. Standard additions of Nicotine were carried out from Nicotine standard samples. Standard additions of urine were carried out from a solution containing NIC in 23 mL of B–R buffer pH 2 and 1.0mM sodium dodecylsulfate in the voltammetric cell and analyzed under same conditions as used to obtain calibration graph.

2.6. Analysis of cigarettes samples.

Cigarettes were taken out of their rolling paper and dried for 30 minutes at 40°C oven before weighing. 0.1 g from a cigarette tobacco mixture of ten cigarettes taken from two packs of the same brand was placed in a 50mL glass vial with a cap. We add 10mL water using a pipette, and then the contents of the vial were sonicated for 3 h in an ultrasonic water bath and filtered. Appropriate volume (100μL) of the

clear filtrate were mixed with the B-R buffer (pH 2.0) containing 1.0mM sodium dodecylsulfate in the voltammetric cell and analyzed under same conditions as used to obtain calibration graph.[1]

3. Results and Discussion

3.1. Morphologies of the different electrodes.

SEM images of the CPE and CNMCPE are shown in Figure 1A,B, respectively and shows their physical morphology. The SEM image of CPE (Fig. 1A) shows a microstructure with a discontinuous grain growth and also shows the graphite particles are covered by a very thin film of paraffin oil. The SEM image of CNMCPE (Fig. 1B) shows that metallic nanoparticles are located at different elevations over the CPE surface. Moreover, a random distribution and interstices among the nanoparticles were observed in the SEM image of the CNMCPE exhibiting a large random surface area.

The EDX data of the CeO_2 nanoparticles is shown in Fig. 1C, indicates the presence of Ce and O peaks, and confirms that CeO_2 nanoparticles were indeed coated on the electrode surface. These results suggest that CeO_2 nanoparticles were successfully prepared by this simple electrochemical method.

3.2. Electrochemistry of NIC using SDS

Figure 2 compares cyclic voltammograms of 1.0×10^{-3} M NIC in B–R buffer pH 2.0 at a scan rate of 25 mV s^{-1} recorded at three different electrodes i.e. (1) bare CPE, (2) CNMCPE and (3) CNMCPE/1.0 mM SDS. At bare CPE there is no oxidation peak observed, while the electrodeposition of Ce-nanoparticles onto the surface of the CPE (CNMCPE) was an effective strategy to enhance the detection of NIC, where CPE represent the best electrode type for Ce-nanoparticles electrodeposition, because of no adsorption of Ce^{3+} or Ce^{4+} and formation of oxides

on the surface of graphite electrodes.[19] Cerium dioxide (CeO_2) is the most stable oxide of cerium. This compound is also called ceria or ceric oxide.[22]

The surfactant has two important roles, firstly is that it can stabilize radical ions and other reaction intermediates, which effect on the mechanism of the electrode reaction. Secondly, it modifies the double layer structure.[1] The sensitivity of CNMCPE/SDS for NIC determination was clearly increased being an indicative that the rate of electron transfer was increased. The surfactant-modified electrode sensitivity was about 2.45 times higher than CNMCPE. Nicotine exists as a positively charged protonated form under the studied pH condition (pH 2.0).[23] On the other hand, the SDS adsorption onto electrode surface forms a negatively charged hydrophilic film oriented towards the water bulk phase. Based on this fact, positive charged nicotine has a tendency to accumulate in the negatively charged crown of anionic SDS micelles, which may increase the electron transfer rate.[24]

3.3. Effect of pH.

The effect of pH was evaluated for CNMCPE/SDS using B–R buffers within the pH range of 2.0–8.0 (Fig. 3). The anodic peak potentials shifted negatively with the increase in the pH, indicating that the electrocatalytic oxidation of NIC at the CNMCPE/SDS is a pH-dependent reaction showing that protons have taken part in their electrode reaction processes. Even though the exact oxidation mechanism of nicotine has not been determined up to now, according to a hypothesis proposed by Suffredini et al.[10] oxidation mechanism in alkaline solutions at boron-doped diamond electrode involves the formation of methanol and substitution of the CH_3 to OH in the tertiary nitrogen of pyrrolidine ring with two electron transitions.

The highest oxidation peak current was obtained at pH 2 (inset), then the peak current decreased from pH 2.0 to pH 5.0 and increased again up to pH 8.0. Nicotine is

a weak diacidic base having two pKa values, pKa_1 = 8.02 and pKa_2 = 3.12 which correspond to the protonation of pyrrolidine nitrogen (monoprotanated form) and pyridine nitrogen (diprotonated form) present in nicotine molecule, respectively.[23]These results strongly prove that the oxidation step of nicotine is located on the pyrrolidine ring and attributed to the oxidation of tertiary nitrogen.

3.4. Effect of scan rate.

Cyclic voltammetry experiments were carried out as a function of scan rate to give information related to the adsorptive properties of the reaction studied. A plot of I_{pa} vs. $\upsilon^{1/2}$ (υ ranging from 10 to 100 mV s^{-1}) for 1.0 × 10^{-3} M NIC using CNMCPE/SDS in B–R buffer (pH 2.0) gave a straight line relationship. The linearity of the relationship indicated a diffusion controlled mechanism and that the adsorption of aggregates at the electrode surface was also possible. Typical CV curves of NIC at different scan rates were shown in figure 4. The oxidation peak currents increased linearly (inset) with the regression coefficient r^2 = 0.9997& γ = 5) for respectively, suggesting that the reaction is diffusion-controlled electrode reaction.

The relation between the anodic peak current and scan rate has been used to evaluate the ‘‘apparent’’ diffusion coefficient, D_{app}, for studied compounds. D_{app} values were calculated from the Randles Sevcik equation.[25]

$$\mathbf{I_{pa} = 0.4463\ nFAC_0\left(nF\upsilon D/RT\right)^{1/2}} \qquad (1)$$

In this equation: i_{pa} is the maximum current (A), n is the number of electrons transferred in the redox event, C_0 is the analyte concentration (1 × 10^{-6} mol cm^{-3}), A is the electrode area in cm^2, D is the electroactive species diffusion coefficient (cm^2 s^{-1}), ν is the scan rate in V/s, F is Faraday Constant in C mol^{-1}, T is the temperature in K and *R* is the Gas constant in VC K^{-1} mol^{-1}

The apparent diffusion coefficients, D_{app}, of NIC using CNMCPE and CNMCPE/SDS in B–R buffer (pH 2.0) were calculated from cyclic voltammetry (CV) experiments and were found to be 4.195×10^{-5} cm^2 s^{-1} and 7.189×10^{-5} cm^2 s^{-1}, respectively; this indicates that the redox reaction of the analyte species takes place at the surface of the electrode under the control of the diffusion of the molecules from solution to the electrode surface.

3.5. Effect of accumulation time

In order to investigate the response of CNMCPE/SDS, the CV for 1.0×10^{-3} M NIC in B–R buffer (pH 2.0) solution were recorded every three minutes (Fig. 5). It was found that the anodic peak currents increased with increasing the accumulation time. The highest current response for CNMCPE was reached after 21 minutes at 1.0 V vs. SCE, so the optimum time for electrode stability is 21 minutes. Repetitive measurements indicated that this electrode has good reproducibility and stability during the voltammetric measurements.

3.6. Electrochemical impedance spectroscopy (EIS) measurements

Electrochemical impedance spectroscopy (EIS) is an effective tool for studying the interfacial properties of surface-modified electrodes.[26] The impedance plots are shown as both Bode (Fig. 6a,b) and Nyquist plots (Fig. 7a,b), respectively. The Bode and Nyquist plots for the CNMCPE at 1×10^{-3}M NIC solution only (Fig.6a,7a) and CNMCPE/SDS at 1×10^{-3}M NIC solution (Fig.6b,7b), respectively. The Nyquist plots include a small semicircle corresponding to charge transfer resistance and a linear part corresponding to diffusion process. The impedance data were thus simulated to the appropriate equivalent circuit for the cases exhibiting two time constants (Scheme 2). This simulation gave a reasonable fit with 1% average error. The appropriate equivalent model used to fit the high and low frequency data consists of two circuits in series from Z_wCPE_1 and $R_{CT}CPE_2$

parallel combination and both are in series with R_s. CPE_1 is related to the constant phase element (CPE) of the capacitance of the inner layer and CPE_2 to the outer layer, while R_{CT} is the charge transfer resistance of the outer layer related to the small semicircle at high frequency.[27, 28] Z_w is a Warburg component related to the linear region at the lower frequencies in the Nyquist plot which is related to diffusion phenomena.[29, 30] The experimental data were fitted using Thales software provided with the workstation where the dispersion formula suitable to each model was used.[27,30] In this complex formula an empirical exponent (α = 0 to 1) is introduced to account for the deviation from capacitive ideality behavior due to surface roughness.[31, 32] An ideal capacitor corresponds to α = 1 while α = 0.5 becomes the CPE in a Warburg component.[29] In all cases, good conformity between theoretical and experimental results was obtained with an average error of 1%.

Table 1 lists the best fitting values calculated from the equivalent circuit for the impedance data at the two different cases for the CNMCPE. The value of solution resistance, R_s, for each pH value was almost constant within the limits of the experimental errors. CNMCPE/SDS shows relatively higher values for the capacitance or lower values for the impedance compared to CNMCPE indicating a more conducting behavior due to electrode surface ionic adsorption by SDS. Also the same is observed for Z_W values, where it has higher values for CNMCPE/SDS than for CNMCPE. Also, the lowest R_{CT} or highest CPE values obtained at pH = 2 for both tested electrodes indicated higher conductivity and confirming highest oxidation peak current obtained from CV's results.

Z_W is characterized by a very low frequency slope of -0.5 and it intercept on the log Z axis at f = 1 Hz of $\sigma\pi^{-1/2}$, where σ is the Warburg impedance coefficient (ohm cm^2 $s^{-1/2}$) [33, 34]

$$\log Z = \log \sigma \pi^{-1/2} - \tfrac{1}{2} \log f \qquad (2)$$

σ can be obtained from equation (2) by getting log Z values at f = 1 which is 2.208 and 2.176 for both CNMCPE and CNMCPE/SDS at pH = 2, respectively. σ values are evaluated as 286.25 for CNMCPE and 266.17 for CNMPE/SDS, this means that diffusion processes take place on the electrode. Diffusion coefficient at pH = 2 can be calculated using the following equation:[35]

$$D = \left[\frac{RT}{\sqrt{2}\, AF^2 \sigma C} \right]^2 \qquad (3)$$

where D is the diffusion coefficient ($cm^2\ s^{-1}$), A is the area of the electrode (cm^2), σ is Warburg coefficient (ohm $cm^2\ s^{-1/2}$), C is the concentration of nicotine (mol cm^{-3}), R is the gas constant, J K^{-1} mol^{-1}, T is the temperature (K) and F is Faraday constant (C mol^{-1}).

D is found to be equal 8.65 x 10^{-5}, for CNMCPE and 10.01 x 10^{-5} for CNMCPE/SDS at pH = 2. Thus diffusion coefficient values calculated from EIS measurements is comparable to that obtained from CV's measurements. This confirms well CV's data indicating that the redox reaction of the analyte species takes place under diffusion control process.

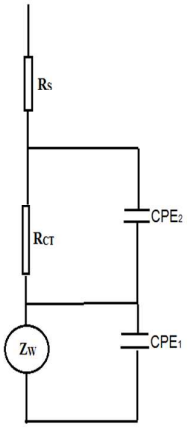

Scheme 2: The used equivalent circuit in the fitting experiments of the EIS.

3.7. Calibration curve

Fig. 8 represent CV data for Calibration experiments processed on CNMCPE for the determination of nicotine using successive additions of 1×10^{-3} M NIC concentration in 0.04M B–R buffer pH 2.0 containing 1mM SDS solution (optimized conditions) and scan rate of 10 mV s^{-1}.

Method on CNMCPE represents specific and well defined concentration dependence as the CNMCPE showed a highly fast and sensitive response to the change of NIC concentration. Fig. 8.inset represents Calibration curve obtained by successive additions of nicotine over 4.0×10^{-6} to 5.0×10^{-4} M concentration ranges at which the electrode provided a linear response toward NIC with correlation coefficient of 0.999. The concentration of NIC was calculated from the linear regression equation of the standard calibration curve: i_{pa} (μA) = 0.023 C (M) + 0.5886.

The sensitivity of the proposed method was evaluated both the limit of detection (LOD) and limit of quantification (LOQ) values. The LOD and LOQ were calculated using the following equations:

$$LOD = 3s/b \qquad (4)$$

$$LOQ = 10s/b \qquad (5)$$

where s is the standard deviation of the oxidation peak current (three runs) and b is the slope (μA/M) of the related calibration curves, and they were found to be 9.43×10^{-8}M and 3.14×10^{-7}M respectively.

3.8. Comparison of several methods for the determination of NIC

Comparisons of the data obtained for NIC determination by various methods and electrochemical techniques are shown in Table 2[36-39] and Table 3[1,10,12,16,&40], respectively. Compared with other current techniques for the determination of NIC, the CNMCP sensor has some advantages. The sensor has the advantage of using non-

poisonous and lower cost reagents giving well stability although it has nearly the same specific selectivity. The instruments of HPLC, GC, SPE and spectrometry are more sophisticated and expensive than that of the CNMCP sensor. Furthermore, the procedures and pre-treatment for these methods are complicated while that used for CNMCP sensor are very easy and simple.

3.9. Application of CNMCP sensor in urine

Fig. 9 shows the calibration curve for the usage of CNMCP sensor at real samples as urine which gave a straight line on the concentration range of 6×10^{-6} M – 4.8×10^{-4} M. From equation of the calibration curve, Ipa (μA) = 0.0181C (M) + 1.4796, the concentration of NIC in urine samples was calculated. The correlation coefficient, r^2 =0.997, the LOD is 2.06×10^{-7} M and the LOQ is 6.89×10^{-7} M. To ensure the validation of the proposed method in urine samples, table 4 shows the evaluation of the precision and accuracy of the proposed method for the NIC detection for four different concentrations on the calibration curve which are repeated for five times. The recovery, standard deviation, standard error and the confidence level were calculated as well.

3.10. Analysis of real cigarette brands samples

For practical application, two products of different cigarette brands were analyzed (L&M and Marlboro) to ensure the validation of the proposed method at real samples. Ultrasonication method of the tobacco samples which are used in recent studies is considered as an alternative technique otherwise the most commonly methods used for nicotine analysis in tobacco samples which use highly cost and environmentally harmful organic solvents and required complex extraction procedures.[1] The sample extraction efficiency can be greatly increase when the bubbles created by the sonication of solutions was collapsed results in the generation

of high local energy and a high contact between solvent and solute. The method used for the preparation of the sample in this study was a slight modification of the method described by Suffredini et al.[10]. In our study, the ultrasonic extraction time of 3 h was chosen instead of 1 h in order to achieve a quantitative recovery of nicotine into aqueous solution. The precision and accuracy of the method can be tested from the results obtained in the analysis of different cigarette samples shown in Table 5. In practice it is necessary to know that the nicotine reported in the cigarette packs correspond to the amount of nicotine which could be absorbed by the smoker when he smokes the cigarette in standard conditions.

In our study we made the spike/recovery experiments in order to test the validation of the proposed method. Recovery studies were performed by adding the appropriate volume of standard nicotine solution prepared in supporting electrolyte to the nicotine content previously determined at the tobacco sample. Comparing the concentration obtained from the spiked mixtures with those of the pure nicotine we were able to calculate the nicotine recovery. The recovery data ensure the accuracy of the voltammetric detection of nicotine in tobacco as it was found that nicotine amounts can be quantitatively recovered by the proposed method.

Due to the low concentration level of other minor alkaloids (0.2–0.5 % of total alkaloids) which can not affect the accuracy of nicotine detection at the sensitivity level of voltammetric measurements, the interference of alkaloids which may be present in tobacco was not performed in this study [4].

4. Conclusions

Through the present study we have introduced a sensor based on CP electrode modified with cerium nanoparticles was used for electrochemical determination of NIC. The advantages of the cerium nanoparticles enhanced the sensitivity of the CP

electrode significantly. The experimental conditions such as pH, scan rate, accumulation time and the deposition time were studied to find the highest sensitivity for the determination of NIC. Under the optimum conditions, calibration plots for NIC were linear in the ranges of 4.0×10^{-6} to 5.0×10^{-4} M with correlation coefficients of 0.999 and detection limits of 9.43×10^{-8} M. The results showed that the method was very easy and simple with enough sensitivity and selectivity for NIC detection in cigarettes and urine samples with satisfactory results.

.

References

[1] A. Levent ,Y. Yardim and Z. Senturk, *Electrochim. Acta*, 2009, **55**, 190-195.

[2] D.J. Doolittle, R. Winegar, J.K. Lee, W.S. Caldwell, A. Wallace, J. Hayes and J.D. deBethizy, *Mutat. Res.* 1995, **344**, 95-102.

[3] M. Chena, M. Alegrea, A. Durgavanshib, D. Bosec and J. Romero, *Journal of Chromatography B,* 2010, **878**, 2397-2404.

[4] J.M. Garrigues, A. Perez-Ponce, S. Garrigues and M. de la Guardia, *Chim. Acta*, 1998, **373**, 63-71.

[5] H. Omara and S. Attaf, *World Journal Of Pharmacy And Pharmaceutical Sciences,* 2014, **3**, 1327-1340.

[6] R.C. Gupta and G.D. Lundberg, *Clin. Toxic*, 1977, **11**, 437-442.

[7] Å. Zander, P. Findlay, T. Renner and B. Sellergren, *Anal. Chem*., 1998, **70**, 3304-3314.

[8] C.E. Efstathion, E.P. Diamandis and T.P. Hadjiioannon, *Anal. Chim. Acta*, 1981, **127**, 173-180.

[9] S.M. Saad and E.M. Elnemma, *Analyst*, 1980, **114**, 1033-1037.

[10] H.B. Suffredini, M.C. Santos, D. De Souza, L. Codognoto, P. Homem-de-Mello, K.M. Honorio, A.B.F. Da Silva, S.A.S. Machado and L.A. Avaca, *Anal. Lett*., 2005, 38, 1587-1599.

[11] A. Hannisdal, Q. Mikkelsen, K.H. Schroder and Collect. Czech., *Chem. Commun.*, 2007, **72**, 1207-1213.

[12] Y. Yang, M. Yang, H. Wang, L. Tang, G. Shen and R. Yu, *Anal. Chim. Acta*, 2004, 5**09**, 151-157.

[13] C.-T. Wu, P.-Y. Chen, J.-G. Chen, V. Suryanarayanan and K.-C. Ho, *Anal. Chim. Acta*, 2009, **633**, 119-126.

[14] M.S. Lin, J.S. Wang and C.H. Lai, *Electrochim. Acta*, 2008, **53**, 7775-7780.

[15] M. J. Sims, N. V. Rees, E. J.F. Dickinson and R. G. Compton, *Sensors and Actuators*, 2010, **B 144**, 153-158.

[16] C.T. Wu, P.Y. Chen, J. G. Chen, V. Suryanarayanan and K. C. Ho*, Analytica Chimica Acta*, 2009, **633** ,119-126.

[17] Ľ. Švorc , D. M. Stanković and K. Kalcher, *Diamond & Related Materials*, 2014, **42**, 1-7.

[18] H. Liu, etal, *Electrochem.Comm.*, 2005,**7**, 1357-1363.

[19] Z. Xie, Q. Liua, Z. Changa and X. Zhang, *Electrochim. Acta*, 2013, **90**, 695-704.

[20] S. Liu, J. Li, S. Zhang and J. Zhao, *App. Surf. Sci.*, 2005, **252**, 2078-2084.

[21] N.K Chaki and K. Vijayamohanan, *Biosens. Bioelectron*., 2002, **17**, 1-12.

[22] Q. Wang, anodic electrochemical synthesis and characterization of nanocrystalline cerium oxide and cerium oxide/montmorillonite nanocomposites, Dissertation Prepared for the Ph. D., university of north Texas, 2008.

[23] S.S. Yang and I. Smetana, *Chromatographia*, 1995, **40**, 375-378.

[24] X.L. Wen, Y.H. Jia and Z.L. Liu, *Talanta*, 1999, **50**, 1027-1033.

[25] N. Yang, Q. Wan and J. Yu, 2005, **110**, 246–251.

[26] W. Zhang, G. Xie, S. Li, L. Lu and B. Liu, *App. Surf. Sci*., 2012, **258**, 8222-8227.

[27] A.M. Fekry, *International Journal of Hydrogen Energy*, 2010, **35**, 12945-12951.

[28] M.A. Ameer, A.M. Fekry, *Progress in organic coatings*, 2011, **71**, 343-349.

[29] F. El-Taib Heakal and A.M. Fekry, *J. of Electrochimical society*, 2008, **155**, C534-C542.

[30] F. El-Taib Heakal, A.M. Fekry and M.Z. Fatayerji, *J. of Appl. Elect*., 2009, **39**, 1633-1642.

[31] U. Retter, A. Widmann, K. Siegler and H. Kahlert, *Journal of Electroanalytical Chemistry,2003,* **546**, 87-96.

[32] Mackdonald DD, "Transient Techniques in Electrochemistry", Plenum Press, New York, Ch. 6. 1977.

[33] G.W. Walter, *Corros. Sci.* 1986, **26**, 681-703.

[34] M.A. Ameer, *Materials and Corrosion*, 2000, **51**, 242-246.

[35] R. Vedalakshmi, V. Saraswathy, Ha-Won Song and N. Palaniswamy, Corrosion Science, 2009, 51, 1299–1307

[36] A.–Z.C. Gudet and P. Buri, *Pharm. Sci.*, 1998, **8**, 139–144.

[37] G.H. Lu and S. Ralapati, *Electrophoresis*, 1997, **19**, 19–26.

[38] M.T. Xu, R.F. Qi and Q.M. Gao, Photometric determination of nicotine in tobacco with bromcresal green, *Lihua Jianyan, Huaxue Fence*, 1998, **34**, 1-78.

[39] J.M. Garrigues, A. Perez-Ponce, S. Garrigues and M. de la Guardia, *Analyst*, 1999, **124**, 783-786.

[40] A. Geto, M. Amare, M. Tessema and S. Admassie, *Electroanalysis* **, 24**, 659–665.

Table.1: Electrochemical impedance fitting parameters.

Electrode	pH	R_s /Ωcm^2	Z_w /$k\Omega\ cm^2 s^{-1/2}$	CPE_1 /$\mu F\ cm^{-2}$	α_1	R_{CT} /$k\Omega\ cm^2$	CPE_2 /$\mu F\ cm^{-2}$	α_2
CNMCPE	2.0	163	153.2	0.34	0.55	1.27	30.85	0.86
	5.0	142	49.81	0.12	0.64	1.88	19.44	0.87
	8.0	170	70.99	0.31	0.60	1.49	22.40	0.94
CNMCPE/SDS	2.0	148	562.8	0.49	0.50	0.87	62.34	0.78
	5.0	126	201.1	0.13	0.60	1.45	37.09	0.91
	8.0	112	552.2	0.43	0.54	1.13	57.48	0.91

*R_s: the solution resistance, Z_w: Warburg impedance, CPE: Constant phase element, α: correlation coefficients, R_{CT}: charge transfer resistance.

Table. 2: Comparison of the CNMCP sensor with other methods for the determination of NIC.

Method	Calibration range (M)	Detection limit (M)	Reference
HPLC	6.8×10^{-6}-3.4×10^{-5}	6.2× 10-7	[36]
CE	8.1×10^{-6}-8.1×10^{-5}	3.8×10^{-7}	[37]
Spectrometry	up to 7.4×10^{-5}		[38]
Flow injection	0 - 5.8×10^{-2}	6.2×10^{-7}	[39]
CNMCP sensor	4.0×10^{-6}-5.0×10^{-4}	9.4×10^{-8}	This work

Table. 3: Comparison of the CNMCP sensor with different modified electrodes for the determination of NIC.

Method	Calibration range (M)	Detection limit (M)	Reference
Pencil graphite electrode	7.0×10^{-6}-1.07×10^{-4}	2.0×10^{-6}	[1]
BDD	5.0×10^{-6} - 5.0×10^{-4}	3.1×10^{-6}	[10]
Cho enzyme biosensor	9.2×10^{-5}-2.0×10^{-4}	1.0×10^{-5}	[12]
TiO_2/MI-PEDOT	0 - 5.0×10^{-3}	4.9×10^{-6}	[16]
p-(AHNSA/GCE)	1.0×10^{-6} -2.0×10^{-4}	0.87×10^{-6}	[41]
CNMCP sensor	4.0×10^{-6}- 5.0×10^{-4}	9.4×10^{-8}	This work

Table 4: The precision and accuracy of the CNMCP sensor for NIC detection in urine sample

[NIC] added (M) x 10^{-6}	[NIC] Found[a] (M) x 10^{-6}	Recovery (%)	SD x 10^{-6}	S.E[b] x 10^{-6}	C.L.[c] x 10^{-6}
12.00	12.03	100.2	0.05	0.02	0.08
60.00	60.20	100.3	3.61	0.18	0.58
120.0	119.77	99.80	0.22	0.11	0.35
300.0	299.25	99.75	1.70	0.85	2.77

[a] Mean for five determinations [b] Standard error = $SD/n^{1/2}$ [c] Confidence at 95% confidence level

Table 5: The recovery analysis of nicotine in cigarette tobacco.

Cigarette Brand	[Nic.] taken×10^{-6}M	[Standard] added ×10^{-6}M	Found×10^{-6}M	Recovery (%)
L&M	60.00	**60.00**	120.26	100.22
	120.00	-	179.83	99.91
	180.00	-	239.69	99.87
	240.00	-	300.13	100.04
Marlboro	60.00	-	120.30	100.25
	120.00	-	180.06	100.03
	180.00	-	239.98	99.99
	240.00	-	300.19	100.06

Figures Captions

Figure.1. SEM images for (A) CPE and (B) CNMCPE and EDX spectra of CeO_2 nanoparticles.

Figure 2. CVs of bare CPE, CNMCPE and CNMCPE/SDS in B–R buffer pH 2.0 containing 1.0×10^{-3} M NIC at 25 mV s^{-1}.

Figure 3. CVs of CNMCPE/SDS in B–R buffer of different pH values containing 1.0×10^{-3} M NIC.

Inset: Variation of anodic peak current (I_{pa}) for CNMCPE and CNMCPE/SDS values with pH values.

Figure 4. CVs of CNMCPE/SDS in B–R buffer of pH 2.0 containing 1.0×10^{-3} M NIC at different scan rates.

Inset: Variation of anodic peak current (I_{pa}) with the square root of the scan rate ($\upsilon^{1/2}$) for CNMCPE and CNMCPE/SDS

Figure 5. Variation of anodic peak current (I_{pa}) with different accumulation times : (1 – 40 minutes) of CNMCPE in B–R buffer pH 2.0 containing 1.0×10^{-3} M NIC.

Inset: The CVs of B–R buffer (pH 2.0) solution containing 1.0×10^{-3} M NIC recorded every three minutes.

Figure. 6. Bode plots of NIC for (a) CNMCPE, (b) CNMCPE/SDS at different pH values.

Figure.7. Nyquist plots of NIC for (a) CNMCPE, (b) CNMCPE/SDS at different pH values.

Figure 8: The CVs of successive addition of NIC and 1.0 mM SDS in B–R buffer pH 2.0 at scan rate 10 mV/s using CNMCPE/SDS.

Inset shows the corresponding calibration curve of NIC.

Figure 9: Calibration curve of NIC in urine.

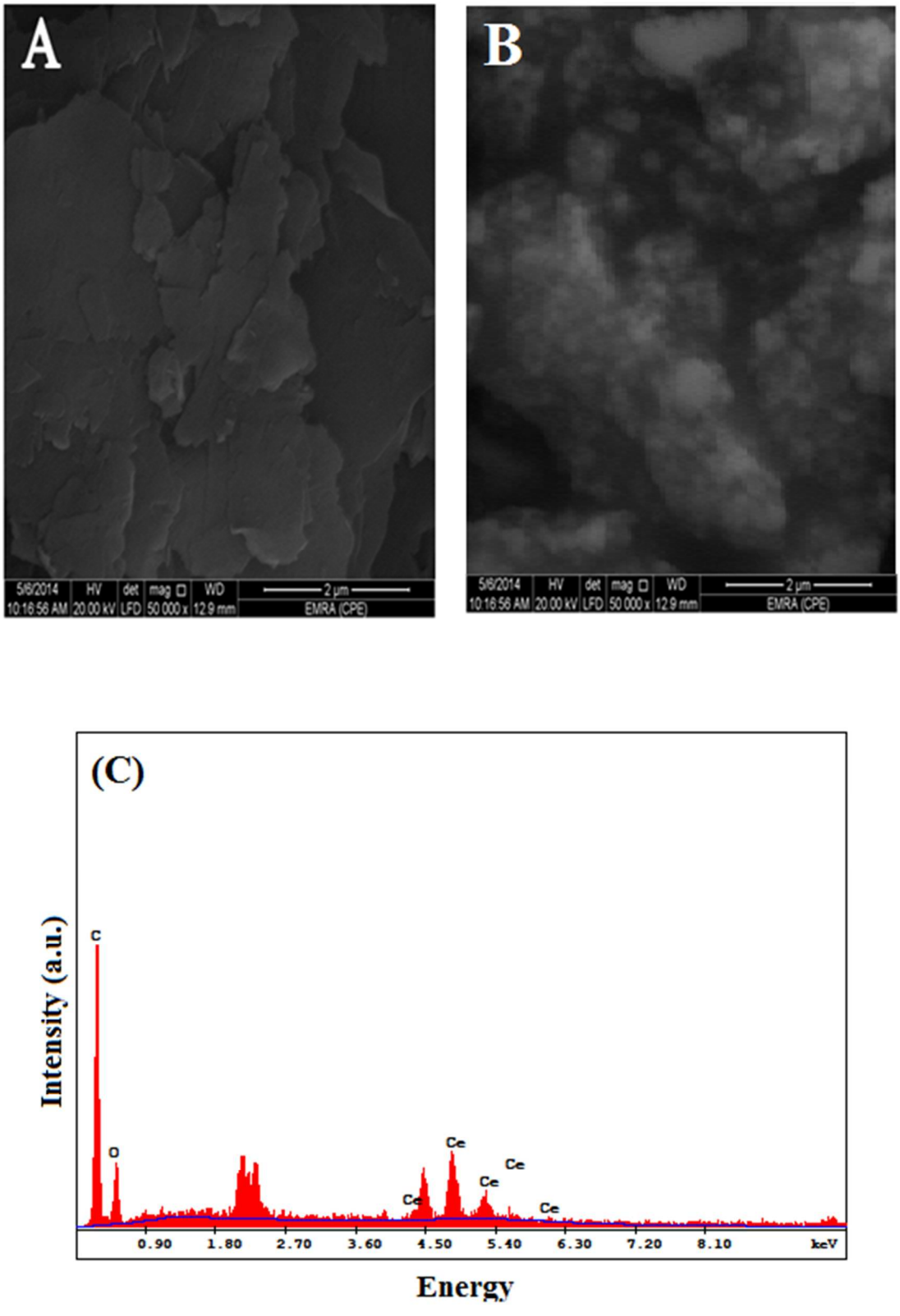

Fig.1A-C

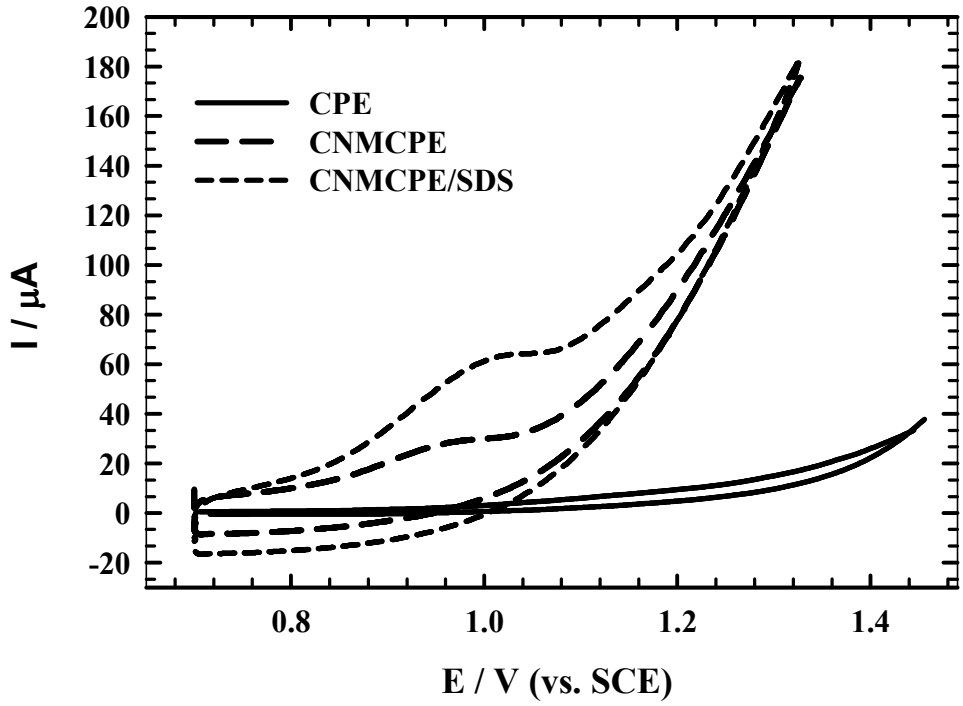

Fig.2

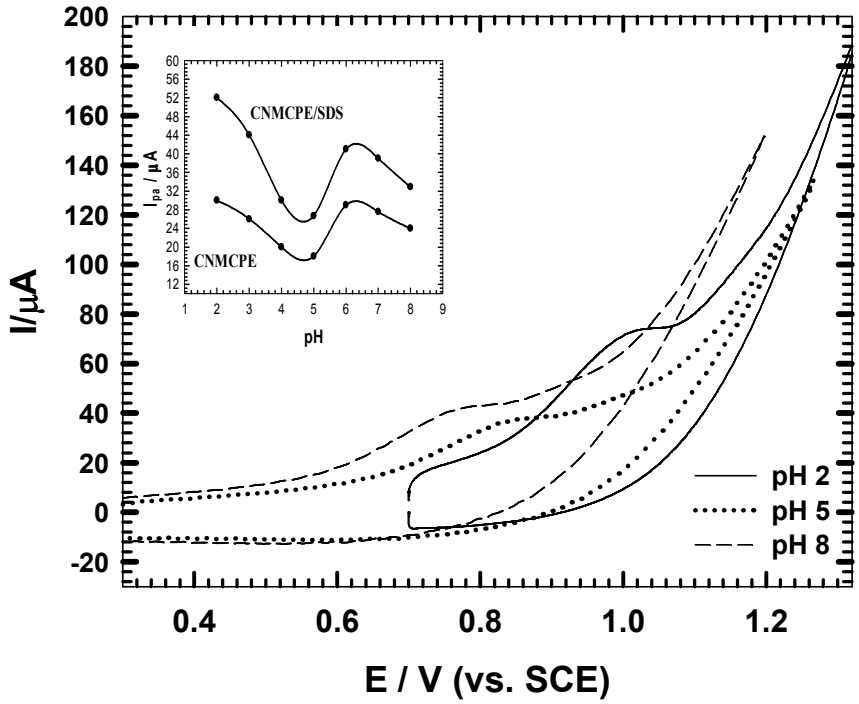

Fig. 3

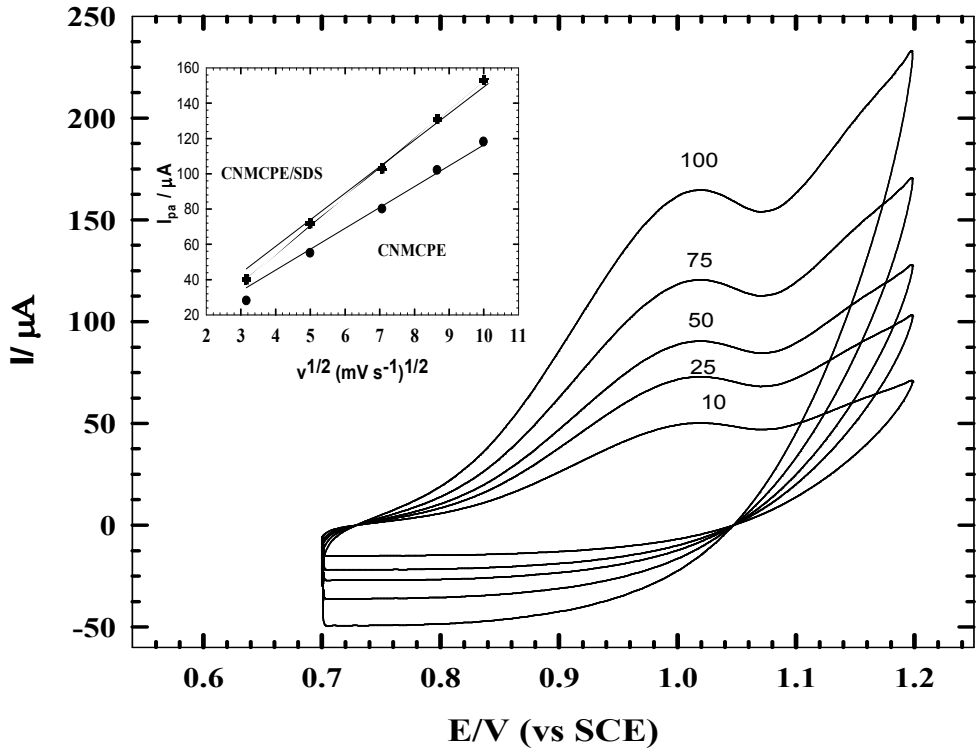

Fig. 4

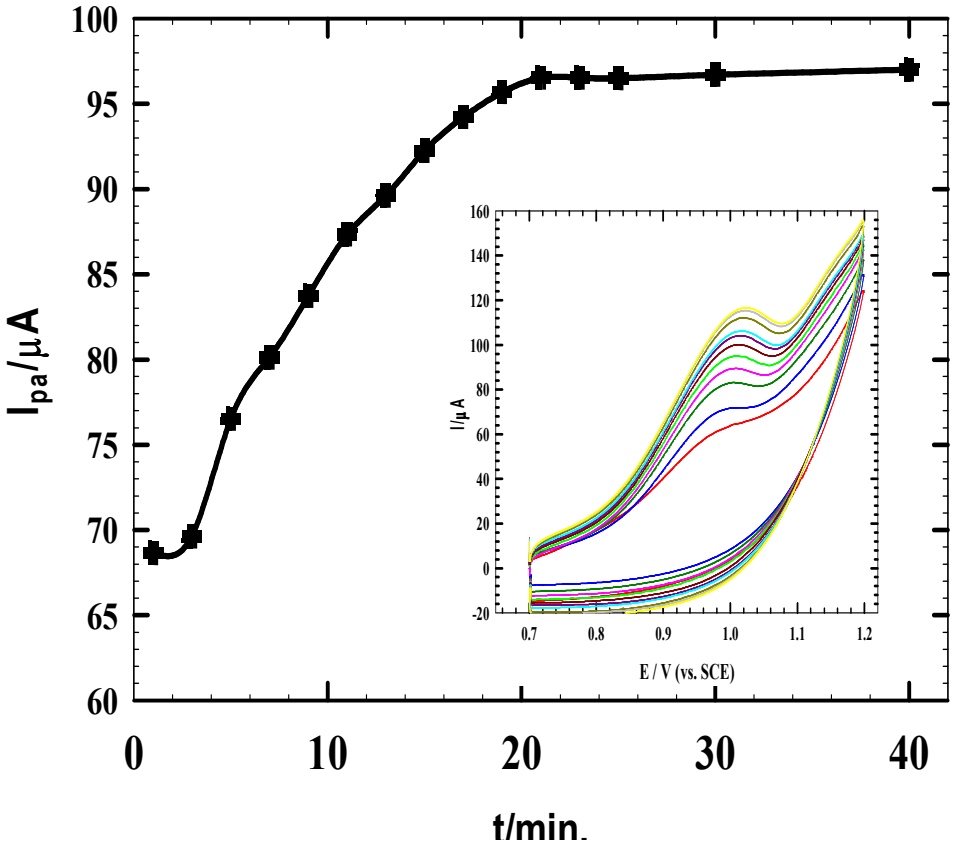

Fig. 5

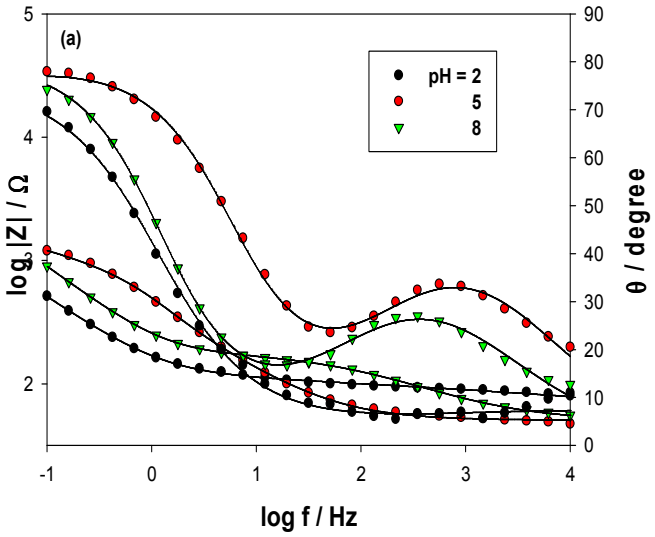

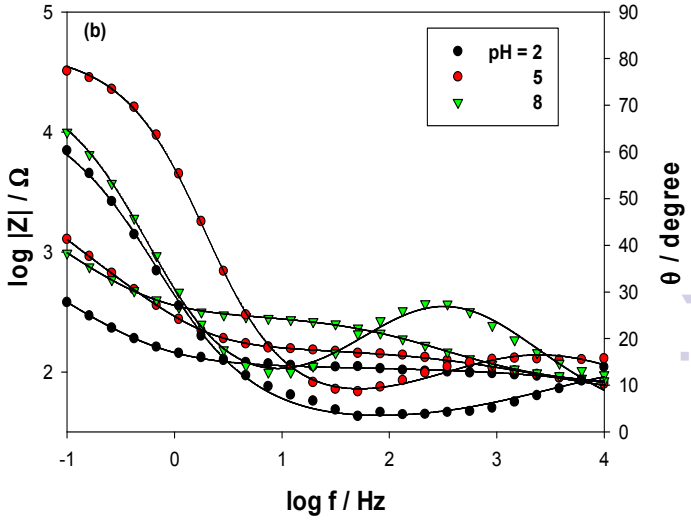

Fig. 6.

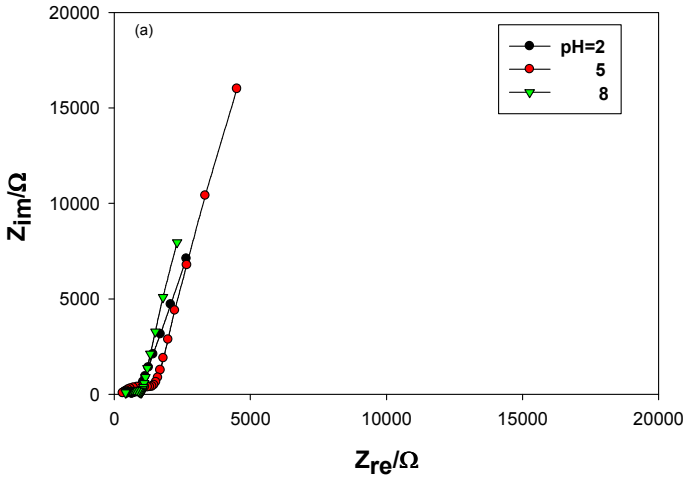

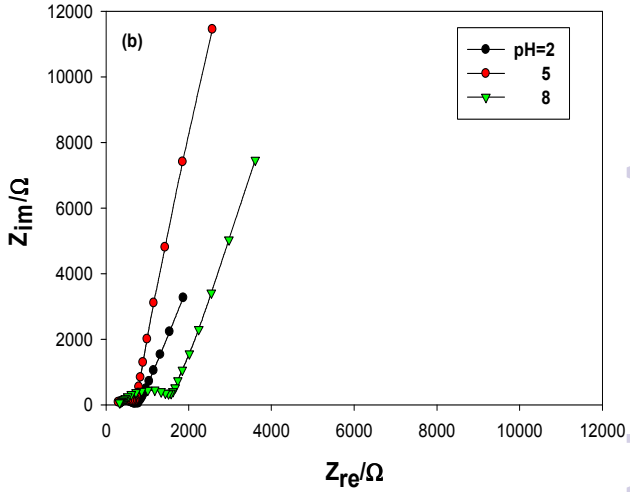

Fig.7.

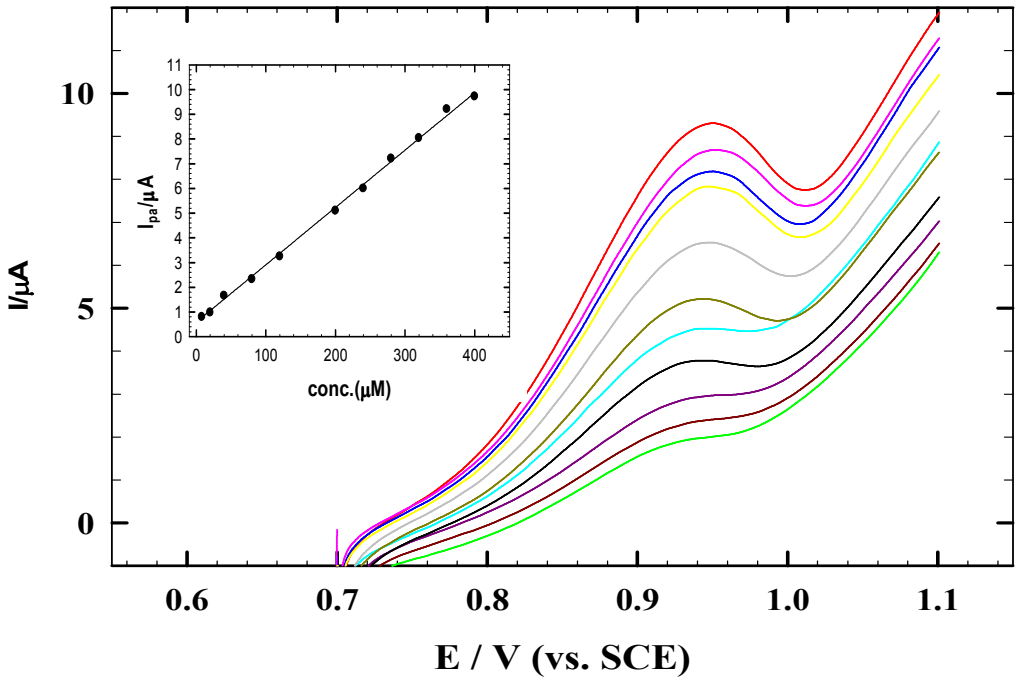

Fig. 8

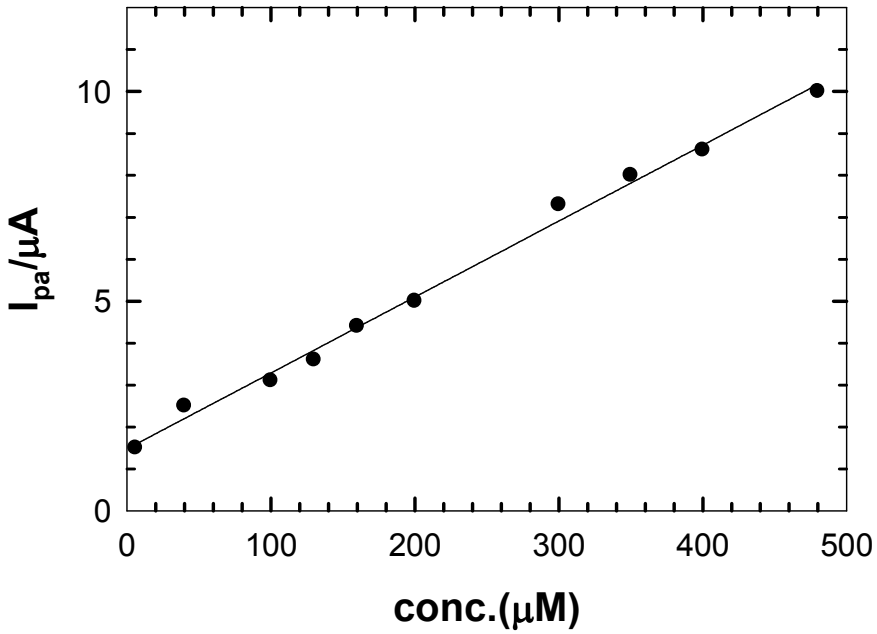

Fig. 9